Oxford Poverty & Human Development Initiative (OPHI)
Oxford Department of International Development
University of Oxford

OPHI RESEARCH IN PROGRESS SERIES 70a

Measuring the Overlap between Climate Hazards and Multidimensional Poverty: A Global Sub-National Assessment

Sabina Alkire*, Nabamallika Dehingia**, Beatriz Jambrina-Canseco*, Niall Maher* and Ricardo Nogales***

October 2025

Abstract
Climate hazards and multidimensional poverty reinforce each other but their interaction remains poorly understood. This paper addresses this by providing the first globally comparable subnational analysis of where multidimensional poverty and climate hazards overlap. To conduct this analysis, the 2025 Global Multidimensional Poverty Index is combined with gridded data on four hazards (high heat, drought, floods, and air pollution) for 1657subnational regions in 108 developing countries. The results suggest a strong contemporaneous overlap between multidimensional poverty and climate hazard exposure. Approximately 78.8% of the multidimensional poor, representing 887 million people, live in regions exposed to climate hazards. More than half of poor people live in regions experiencing two or more hazards. An estimated 11 million people live in regions experiencing all four hazards simultaneously. The overlap is regionally concentrated; South Asia and Sub-Saharan Africa together account for more than 700 million poor people living in regions experiencing climate hazard exposure. Forward-looking projections demonstrate that the countries with the highest rates of poverty today are the same countries expected to experience the greatest increase in exposure to extreme heat in the future. Three insights can be gathered from this analysis: subnational analysis can identify heterogeneity hidden at the national level, multidimensionally poor people's exposure to multiple climate hazards is common globally, and future climate risks are distributed asymmetrically, with risks falling most heavily on countries where poor populations are most exposed. These findings highlight the urgency of integrating climate and poverty analyses to understand these mutually reinforcing phenomena.

---

* Oxford Poverty and Human Development Initiative (OPHI), University of Oxford.
** Human Development Report Office, United Nations Development Programme (UNDP).
*** Oxford Poverty and Human Development Initiative (OPHI), University of Oxford, and Universidad Privada Boliviana. Corresponding author ricardo.nogales@ophi.org.uk

This paper is part of the Oxford Poverty and Human Development Initiative's Research in Progress (RP) series. These are preliminary documents posted online to stimulate discussion and critical comment. The series number and letter identify each version (e.g. paper RP1a after revision will be posted as RP1b) for citation.

For more information, see **www.ophi.org.uk**.

Keywords: Multidimensional Poverty Index (MPI); multidimensional poverty; climate hazards; subnational analysis.

JEL classification: I32, Q54, Q56, R11.

Acknowledgements:
We are grateful to UCLouvain/CRED (EM-DAT), ECMWF Copernicus (ERA5 reanalysis and CAMS EAC4), the World Bank Climate Change Knowledge Portal, UNDP Human Climate Horizons, and FAO/EC-JRC GAUL for data access. Any errors remain our own.

Funding information: This research did not receive any specific grant from funding agencies in the public, commercial, or not-for-profit sectors.

Citation: Alkire, S., Dehingia, N., Jambrina-Canseco, B., Maher, N. and Nogales, R. (2025). 'Measuring the overlap between climate hazards and multidimensional poverty: A global sub-national assessment', OPHI Research in Progress 70a, Oxford Poverty and Human Development Initiative (OPHI), University of Oxford.

1. Introduction

Climate hazards and persistent multidimensional poverty are not parallel crises; but to what extent are they mutually reinforcing phenomena that interact across space and time to deepen and prolong human deprivation? While studies have overlaid monetary poverty and climate at the national level (Winsemius et al, 2018), such analyses are relatively uncommon. National aggregates have helped raise awareness about both problems; however, they obscure the critical fact that the risks and consequences of environmental stressors are highly unevenly distributed within countries. Furthermore, they have focused on monetary, not multidimensional poverty. A finer lens is therefore essential to understand where and how climate hazards overlap simultaneously with the interconnected non-monetary deprivations poor people experience, as captured by the global Multidimensional Poverty Index (OPHI and UNDP 2025, Alkire and Santos, 2014, Alkire et al., 2022).

This paper provides a subnational assessment of the intersection between climate hazards and multidimensional poverty for 1657 subnational regions within 108 developing countries. Our aims are threefold. First, we quantify the number and share of multidimensionally poor people who live in subnational areas exposed, within the same year, to one or more of four environmental hazards, namely high heat, drought, floods, and air pollution. Second, we identify geographic hotspots where multidimensional poverty and climate hazards coincide and where multi-hazard burdens are most pronounced. Third, to illustrate how these findings could be extended across time, we evaluate future heat burdens under alternative emissions scenarios to assess whether countries with higher current poverty are likely to face disproportionate increases in heat stress.

Methodologically, our analysis combines gridded climate and pollution data with the latest release of global MPI data (2025) and estimates mapped to a harmonized administrative geometry in 108 countries. This approach yields a globally comparable, descriptive portrait of exposure at the sub-national administrative level such as states and provinces. Importantly, our mapping exercise of climate and poverty data to subnational units does not claim causal identification. Rather, it provides a spatially explicit diagnostic that surfaces where climate adaptation and poverty-alleviation efforts could be most urgently aligned.

We find that almost 60% of the subnational regions with climate hazard data across the 108 countries experienced at least one of the four hazards in the survey year, and those exposed areas are home to roughly 887 million multidimensionally poor people. This represents approximately 78.8% of the global poor people in the sample. High heat affects the largest share (around 608

million, 54.0%), followed by air pollution (around 577 million, 51.3%), floods (around 465 million, 41.3%) and drought (around 207 million, 18.4%). Overlapping exposure is widespread: around 651 million poor (58%) live in areas facing two or more hazards, and about 11 million live in places experiencing all four hazards. Exposure is regionally concentrated. South Asia accounts for 380 million poor in exposed areas, while Sub-Saharan Africa has 344 million. Future heat burdens are also projected to be unequal. Under a high-emissions pathway, countries in the highest poverty quartile are projected to gain around 37 additional >35°C days per year by 2040–59 and around 92 days by 2080–99.

The remainder of the document presents the data and methodology, reports additional details on our main empirical results, and concludes with a discussion of their implications for policy and future research. In doing so, it demonstrates a methodology that can be applied to other globally comparable datasets, subnationally disaggregated to observe human-climate hotspots. It could also be extended to include other environmental variables and further analyses over time. This analysis is intended to inform policymakers, practitioners, and scholars who require a spatially disaggregated understanding of climate–poverty overlaps to prioritize interventions that are both equitable and effective.

2. Literature Review

The 21st century is increasingly defined by climate change and persistent global poverty. These challenges are widely regarded to be deeply interconnected and mutually exacerbating, with climate change actively undermining development gains and pushing vulnerable populations deeper into overlapping deprivations (see e.g. CRED, 2020). The World Bank (2024) explicitly identifies climate change as a fundamental risk to poverty reduction efforts globally. This recognition highlights the critical urgency of understanding the complex connections between environmental shocks and human well-being more deeply and precisely, so they can be efficiently addressed.

In the connection between climate shocks and poverty, the global Multidimensional Poverty Index (global MPI) can be particularly illuminating as it provides a comprehensive and nuanced understanding of poverty, acknowledging that poverty is not solely about income, but about a lack of access to essential services and opportunities that are fundamental to a dignified life. Indeed, there is a growing academic and institutional research on the intricate relationship between four specific climate shocks—high heat, drought, floods, and pollution—and multidimensional poverty, as measured by the global MPI or its constituent components (Hallegatte et al., 2014; Doan et al., 2023). Making no claim to completeness, we first briefly survey some of the large

literature that addresses climate-poverty linkages, then delve into the specific theoretical connections between each climate shock and multidimensional poverty.

Barrett and Carter (2006, 2013) find that climate change poses a systemic threat that not only slows progress in poverty reduction but actively pushes individuals and communities into persistent states of deprivation, often described as poverty traps. They observe that these traps are characterised by self-reinforcing cycles where recovery from repeated climate disasters becomes increasingly difficult, leading to long-term socioeconomic decline for those that were worse off in the first place. The World Bank (2024) further highlights the development of poverty traps, citing Pakistan's experience with repeated climate disasters that pushed vulnerable groups deeper into poverty. The mechanisms through which these poverty traps operate are critical to understanding their long-term implications on people's lives. Dell et al. (2014) trace how natural disasters directly destroy livelihoods, means of production, equipment, health, services and education infrastructure. The consequences of these losses can extend across generations, as families may pull children out of school, and malnutrition resulting from food deficits may permanently impair cognitive ability and future productivity (c.f. Alderman et al., 2006). While some existing literature explores how climate shocks affect specific dimensions of the MPI, such as nutrition, schooling, and child mortality, no global study has systematically assessed the overlay between subnational multidimensional poverty data and exposure to climate hazards.

Our approach builds on related advances by Hill et al (2025), who combine household survey and spatial hazard data to estimate the population at high risk from climate hazards globally. Their framework provides an important people-centric, threshold-based indicator that combines exposure and vulnerability to identify populations at high risk. We extend on this analysis in two key ways. Firstly, by adopting a multidimensional poverty lens allows for the inclusion of non-monetary deprivations. Secondly, by conducting a spatially explicit subnational analysis that highlights within-country heterogeneity in the overlap between poverty and climate hazards.

A consistent theme across the literature is that poor people bear a disproportionately heavy burden of climate change impacts, despite having contributed the least to the problem (e.g. Hallegatte et al., 2020; Byers et al., 2018). Moreover, this disproportionate impact is not merely a natural consequence of poverty but is causally reinforced by systemic inequalities and policy failures that can amplify their susceptibility to climate shocks (Tonmoy et al., 2014; Hossain et al., 2023). Hallegatte et al. (2020) detail some reasons for this disproportionate impact. First, poor people often reside in climate-risky areas (due to economic opportunities or cheaper living costs). For example, studies on floods demonstrate that overlapping deprivations force households into

hazardous, cheaper locations, representing a significant spatial vulnerability (Silva Araújo et al., 2022; Daniel et al., 2009). Also, they possess less infrastructure for protection and live in communities that tend to lose a greater proportion of their infrastructure during disasters. This exposure is compounded by a lack of protective infrastructure and limited access to insurance, meaning that a single climate shock can wipe out their entire means of living and recovery. Furthermore, inadequate or inequitable government responses and fragmented risk governance often ignore or victimize poor people preventing necessary infrastructure improvements and deepening existing inequalities (Modi et al., 2009). In sum, the poor face disproportionate and systemic exposure to climate risks. We now examine how each hazard specifically relates to multidimensional poverty.

2.1 High heat and Multidimensional Poverty

High heat is often found to be a significant contributor to global mortality and morbidity, with particularly severe effects on vulnerable populations such as pregnant women and infants (Heal and Park, 2016). While individual cases differ, the physiological stress of high heat on the human body tends to exacerbate existing health conditions and can lead to acute heat-related illnesses and increased mortality among children. High heat is estimated to contribute to nearly half a million deaths each year (Zhao et al, 2021). Dimitrova et al. (2024) found that 4.3% of neonatal deaths in 29 low- and middle-income countries (LMICs) between 2001 and 2019 were associated with non-optimal temperatures, with climate change estimated to be responsible for 32% of heat-related neonatal deaths. Pregnancy increases the risk of heat-related illness due to the body's increased effort to cool both mother and baby, making overheating and dehydration more likely (Dimitrova et al., 2024). Infants are particularly vulnerable as their bodies are not yet equipped to regulate heat (Berger et al, 2023).

The detrimental effects of high heat can extend to educational attainment and cognitive development. Physiologically, high temperatures can impair the brain's ability to focus and react, leading to learning loss. For example, evidence from Mexico suggests that a 1 °C higher annual temperature reduces student test scores by 0.07–0.08 SD (Arceo-Gómez and López-Feldman, 2024). This disproportionately impacts poor children in rural areas where schools are more likely to lack temperature controls and students, to lack access to devices for remote learning. Furthermore, temperature significantly influences sleep quality; during heatwaves, infants may experience disrupted sleep, which is linked to emotional and behavioral challenges, disrupted language development, and reduced problem-solving skills in early childhood (Berger et al, 2023).

High heat can significantly affect living standards, through its effect on labor productivity, especially in sectors requiring outdoor or physically demanding work, which are often the primary sources of income for low-income populations. This directly translates into lost wages, reduced capacity for asset acquisition, and a wide range of adverse welfare consequences including impacts on health (Heal and Park, 2016), labor productivity (Sudarshan and Tewari., 2014), and nutrition (Blom et al, 2022). The burden of such consequences of high heat falls disproportionately on low-income communities that face barriers such as unaffordable energy bills, limited access to air conditioning, and lack of protective infrastructure like ventilation, green spaces, and cooling centers.

2.2 Drought and Multidimensional Poverty

Drought is a primary driver of food insecurity, particularly in regions heavily reliant on rain-fed agriculture (UNICEF, 2023). It can lead to devastating crop failures, livestock losses, and subsequent increases in food prices, pushing vulnerable populations into hunger, malnutrition and overall economic distress. Moreover, drought severely limits access to clean and safe water, forcing communities to rely on unsafe sources (WHO, 2024). Globally, an estimated 1 in 4 people lack access to safely managed drinking water (United Nations Children's Fund and World Health Organization, 2024). This scarcity and poor quality of water lead to a surge in waterborne diseases and increased healthcare expenditures, further straining impoverished households.

Importantly, drought is a significant risk factor for child undernutrition, with deep, long-lasting impacts on physical growth, cognitive development, and overall human capital. There is consistent evidence of a negative impact of drought on chronic undernutrition and stunting among children (Seposo, 2025, Lieber et al., 2020). Evidence suggests that the impacts of drought on child growth operate through several interconnected pathways. Health and environmental impacts include reduced water quality and increased exposure to diarrheal disease (Stanke et al., 2013) as well as food insecurity. Income shocks further limit households' ability to invest in child health (Hoddinott, 2006).

2.3 Floods and Multidimensional Poverty

Floods represent one of the most pervasive climate hazards, causing immediate loss of life, widespread destruction of housing, and severe damage to critical basic service infrastructure (Douglas et al., 2008). These direct impacts devastate living standards and compromise physical safety, particularly in vulnerable communities. Rentschler et al. (2022) estimate that 1.81 billion people, or 23% of the world's population, are directly exposed to 1-in-100-year floods.

Moreover, floods create conditions highly conducive to the spread of infectious diseases and inflict significant psychological trauma, leading to both immediate and long-term health crises. Broadly, flooding is associated with outbreaks of diarrheal diseases and undermines the availability of drinking water, leading to scarcer hygienic conditions (Yazdi, 2024). In addition, floods affect economic activities, such as by destroying household assets in low-income settlements (Amoako and Frimpong, 2015). The poor are disproportionately affected by floods due to a confluence of factors, including their residential locations in hazardous areas, lack of protective infrastructure, and limited coping capacities (Hallegatte et al., 2020). This exacerbates existing inequalities and perpetuates a vicious cycle of poverty.

2.4 Pollution and Multidimensional Poverty

Air pollution is a leading global health threat. According to Pozzer et al. (2023), air pollution is estimated to be responsible for over 3 million deaths annually worldwide. Long-term exposure to fine particulate matter ($PM_{2.5}$) significantly increases the risk of respiratory diseases and reduces lung function (Lelieveld et al., 2015; Pozzer et al., 2023). Pollution is a major cause of developmental disabilities, impairing children's health, diminishing their capacity to learn, and reducing their lifetime earnings. Exposure during childhood can permanently damage children's development, with lifelong impacts on health, earnings, and education (Rees et al., 2016).

According to Rentschler and Leonova (2023), low- and middle-income countries account for 80% of people exposed to unsafe $PM_{2.5}$ levels, with 716 million people living in extreme monetary poverty directly exposed to such unsafe conditions. Furthermore, pollution sources, such as industrial plants and transport corridors, are frequently located disproportionately in low-income neighborhoods (Pastor et al., 2001). Together, these dynamics mean that outdoor air pollution not only damages health but also reinforces cycles of poverty and inequality by lowering property values, straining health systems, and reducing the economic opportunities of those most exposed.

Table 1 below summarises how the literature has identified potential interconnections between the four climate hazards in this study and the dimensions that make up the global MPI.

Table 1: A summary: key Pathways through which Climate Hazards may exacerbate Multidimensional Poverty

Climate Hazard	Relation with Health Dimension	Relation with Education Dimension	Relation with Living Standards Dimension
High heat	Neonatal mortality, maternal health complications, heat-related illnesses.	School closures, learning loss, cognitive impairment, disrupted language development, reduced problem-solving skills.	Higher energy costs, reduced asset acquisition capacities via increased medical bills, reduced labor productivity, lost wages.
Drought	Child undernutrition (stunting, wasting), waterborne diseases (diarrhea, cholera), increased medical expenses, crop failure, livestock loss, food price increases, household food insecurity.	School absenteeism (due to illness, water fetching, child labor), reduced enrollment rates.	Asset sales, lost agricultural income, lower access to sanitation and clear water
Floods	Disease outbreaks (cholera, diarrheal diseases), compromised hygiene conditions.	School disruption/closures, lower enrollment rates, higher dropout rates, loss of educational infrastructure.	Housing destruction, asset loss, damage to critical infrastructure (water, power).
Pollution	Respiratory diseases (asthma, lung damage), developmental disabilities in children (reduced IQ, ADHD), increased mortality.	Impaired learning capacity, reduced attention span, school absenteeism due to illness, long-term cognitive impairment.	Increased medical bills, lost productivity/wages, deteriorated living conditions (especially from indoor pollution).

Source: Authors' own compilation.

3. Data and Methods

3.1 Matching MPI data to subnational regions

Our analysis integrates satellite-based climate hazard data with corresponding multidimensional poverty information across sub-national regions in 108 MPI countries. We focus on four hazards – droughts, floods, high heat, and air pollution, aiming to estimate both the number and proportion of multidimensionally poor individuals exposed to these climate threats. This estimation is achieved by spatially mapping both the gridded climate hazard data and the Global MPI estimates to Global Administrative Unit Layers (GAUL) subnational regions.[1]

1 The Global Administrative Unit Layers (GAUL) dataset, developed by the Food and Agriculture Organization of the United Nations (FAO), provides standardized sub-national administrative boundaries. GAUL provides a unified

We employ GAUL administrative boundaries because some of our climate hazard data sources, such as those for heat and floods, are solely reported at the GAUL ADM1 level. GAUL serves as a common spatial reference, allowing us to align datasets that vary in their level of geographic detail. A key step in our analysis therefore included aligning the subnational boundaries used in the Global MPI data with the standardized GAUL ADM1 regions. This process was not without challenges, as the regions defined in the household surveys used to calculate the Global MPI do not always match official administrative units. To resolve these mismatches, we applied different strategies that we describe in Table 2.

Table 2: Methodological challenges and proposed solutions

Methodological Challenge	Our Approach	Implications	Countries/sub-national regions affected
Sub-national MPI data unavailable	Assign national MPI poverty numbers to the sub-national GAUL regions.	Assumes poverty and populations are evenly spread across the sub-national regions within the MPI country.	134 sub-national regions across 7 countries: Armenia, Georgia, Maldives, Montenegro, Seychelles, South Africa, Tuvalu (for Tuvalu, national MPI and national level climate data was used)
Sub-national MPI data available but inconsistent sub-national boundaries for majority of the MPI sub-national areas with GAUL administrative units	Use national MPI and national boundaries for estimating climate data, for four countries with small population size (Kiribati, Nauru, Samoa, Tonga). For the remaining two countries (Trinidad and Tobago and Uzbekistan), assign national MPI poverty numbers to the sub-national GAUL regions.	Assumes poverty and populations are evenly spread across the sub-national regions within the MPI country (for Trinidad and Tobago and Uzbekistan).	Six countries and 33regions; for Kiribati, Nauru, Samoa, and Tonga, we use national estimates of MPI and climate; for Trinidad and Tobago and Uzbekistan, even spread of poverty and population was assumed for 15 and 14 GAUL administrative areas.
Sub-national MPI data available but MPI data less detailed than GAUL ADM1 regions (or example, in Tunisia the MPI survey reported values for "Central West," but the GAUL ADM1 dataset distinguishes the individual provinces of	Assign sub-national MPI poverty numbers to the smaller GAUL regions within the broader MPI area.[2]	Assumes poverty and populations are evenly spread within the larger MPI region.	505sub-national regions across 19 countries

system for country-level (ADM0), first-level (ADM1, e.g., departments or provinces), and second-level (ADM2, e.g., districts) administrative units (Franceschini et al, 2025).

[2] Given China's population size, we disaggregated the national MPI to GAUL ADM1 using provincial populations so headcounts reflect provincial totals. Provincial figures come from the National Bureau of Statistics of China and are harmonized to UNDESA national totals for cross-country consistency.

Kairouan, Kasserine, and Sidi Bouzid.)			
MPI data more granular than GAUL ADM1 regions (For example, The Gambia's Kuntaur and Janjanbureh within GAUL's Central River)	Average population-weighted MPI poverty figures and aggregate total populations to match the broader GAUL ADM1 boundaries.	Some of the finer details present in the original MPI data are lost	42 sub-national regions across 15 countries
Inconsistent boundaries between MPI survey regions and GAUL administrative units	No match	Loss of data.	79 sub-national regions across 37 countries

Source: Authors' own compilation.

The merge with MPI data with each hazard at the region-year level has a high match of 94% and 100% of MPI regions, depending on the hazard. Data for each hazard was dichotomised at the thresholds outlined below into hazard-affected or non-affected regions. The number of concurrent hazards for each region was tracked. The final dataset allows for the computation of the number of MPI-poor populations exposed to each hazard or any number or combination of hazards.

The years of the data are matched at the first year of survey data. Recall that monetary and multidimensional poverty estimations both provide essentially a snapshot of poverty for a given year. The global MPI contains the most recent snapshot of poverty for each included country and subnational region. By overlaying climate hazards for the same year (data for some of which are more continuous), we are identifying the hazards that affected each subnational population in the same period in which certain members of that population experienced poverty. The combined datasets allow for the identification of spatial correlations between climate hazards and multidimensional poverty. The analytical value of this exercise extends to the policy domain. Mapping climate and poverty data together enables the identification of geographic "hotspots" where deprivation and climate vulnerability coincide. These hotspots can serve as priority areas for the allocation of resources in climate adaptation, disaster risk reduction, and social protection programs. Moreover, the resulting maps provide a useful baseline against which future survey waves or projections of climate change impacts can be compared.

3.2. Measuring the climate hazards

3.2.1. Drought Measurement

In our analysis, 'drought' is taken to refer to meteorological drought defined as a sustained period of abnormally low moisture availability (Mishra and Singh, 2010, p. 203). For our measure of drought, we use the 12-month Standardized Precipitation–Evapotranspiration Index (SPEI), which measures the climatic water balance (precipitation minus potential evapotranspiration)

relative to a 30-year baseline (1991–2020). The values in SPEI are expressed as anomalies in standard deviation units: negative SPEI values suggest dry conditions, while positive SPEI values indicate wetter-than-usual conditions (Vicente-Serrano et al., 2010). For our primary SPEI threshold, we classify a region experiencing 'drought' if the annual average SPEI is -1 or lower. Annual average SPEI is calculated from the mean of SPEI values grid within each subnational region. This threshold follows analyses such as the IPCC AR6 Working Group I, where Figures 1-11 identify drought episodes using the same threshold.

Alternative drought indicator datasets were considered but these metrics were evaluated but did not as strong a fit with our analysis. For instance, the Standardized Precipitation Index (SPI) is a measure of drought that existed as a precursor to the SPEI (McKee et al., 1993). Both datasets use measures of standardized precipitation anomalies. However, unlike the SPEI, the SPI does not account for changes in evapotranspiration. If rates of evapotranspiration change over the historical reference period, as do in warming climates affected by climate change, drought will be underestimated (Vicente-Serrano et al., 2010).

It is important to note that the SPEI is a relative measure. A region with an SPEI of −1 may not be in absolute water scarcity if it is typically wet, yet it will still be classified as drought-affected because conditions are drier than its long-term norm. Conversely, chronically arid areas such as the Sahara or Sahel may not register as "in drought" if current conditions align with their 30-year historical mean, even though the arid conditions may still affect their populations in the ways described above. Relative drought measures are standard in the drought studies literature (Vicente-Serrano et al., 2010; IPCC, 2021) and we follow this convention here. However, it should be recognised that maps using this standard drought measure can omit areas in which poverty overlaps with long-term aridity.

We chose to use SPEI as our primary drought measure primarily due to its prominence in the literature and its ease of use. The ERA5 SPEI dataset satisfied our requirements for data coverage and provides consistent global coverage throughout the temporal span of our analysis.

The SPEI data is sourced from the ERA5-Drought dataset, derived from the ERA5 reanalysis (Hersbach et al., 2020; World Bank, 2025), produced by the European Centre for Medium-Range Weather Forecasts (ECMWF). In this dataset, the native spatial resolution is 0.25° × 0.25° (~11 km at the equator), and temporal coverage extends from 1981 to 2024. SPEI is computed from 'precipitation − potential evapotranspiration' values at the grid level, relative to the historical water balance (1991-2020). These grid level values are then averaged across GAUL 2015 administrative boundaries.

Using the primary drought threshold ($SPEI_{12} < -1$), 22.9% of all ADM1–year observations in the global SPEI dataset are classified as being in drought. Figure 1 provides a global map of the regions recorded as being in drought in the latest year that there is matching MPI data available for that region.

Figure 1. Drought exposure by subnational region. Hazard data corresponds to the most recent MPI survey year for each region.

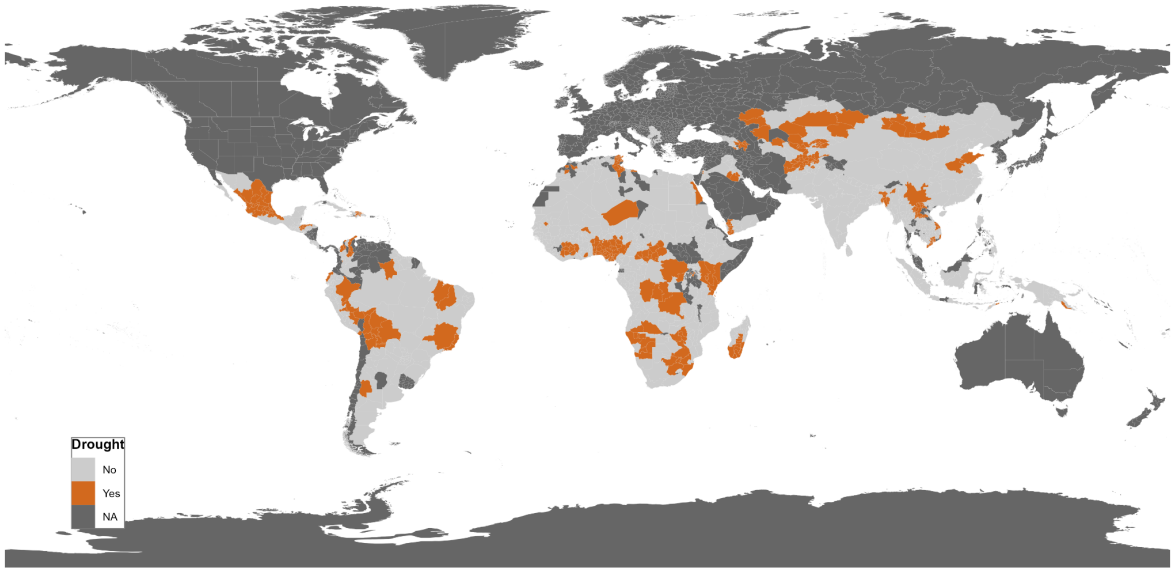

Source: Authors' calculations using ERA5-Drought SPEI (12-month; 1991–2020 baseline) and GAUL 2015 ADM1; matched to Global MPI 2025 region-year.

3.2.2 Heat Measurement

In this analysis, 'high heat' refers to a subnational unit having 30 or more days of daily maximum temperatures equal to or higher than 35 °C in a year. The 35°C threshold definition of 'hot days' is used in the climate literature, such as within the World Bank Climate Change Knowledge Portal, and is consistent with research on human heat tolerance. For instance, Mora et al (2017) demonstrate that lethal episodes can be predicted where mean daily air temperatures are above approximately 37 °C at low humidity and at a lower temperature at higher humidity. Using 35°C as the daily maximum cut-off represents a conservative cut-off at high humidity, while avoiding the need for global humidity data. The >=30 days aspect of the criteria reflects the focus on sustained periods of high heat, which are associated with higher mortality, rather than on isolated heat episodes (Anderson and Bell, 2011).

The heat indicator data comes from the World Bank Climate Change Knowledge Portal, which uses the ERA5 Reanalysis Dataset for generating a range of heat related indicators (Hersbach et al., 2020; World Bank 2025). The ERA5 dataset combines various satellite-derived products into

one global model and can be accessed through the Copernicus Climate Change Service. Via the World Bank Climate Change Knowledge Portal, data is offered at the sub-national level, from 1950 to the present. The spatial aggregation for the heat indicator is carried out through intersection of global data grids with high-resolution polygon boundaries (ADM1 or sub-national level). Weights are assigned to each grid cell based on the fraction of the cell that lay within a particular polygon, which ensures that partially overlapping cells contribute proportionally to the aggregation. Latitudinal weighting is applied to account for the varying areas of grid cells resulting from the Earth's curvature. The area-weighted mean of the measure for heat is then calculated for each polygon or sub-national boundary (World Bank 2025).

This indicator was selected over alternative measures, such as mean annual temperature or percentile-based thresholds, for three reasons. Firstly, it provides a simple and policy-relevant classification globally. Secondly, the threshold captures high heat events, which can be more directly impactful on health than average conditions. Finally, it aligns with other climate indicators in our study by providing clear binary cut-offs. Although measures such as percentile-based measures can adjust for the local climate, the measure we selected can identify absolute temperatures that exceed human physiological tolerance (Mora et al. 2017). For these reasons, the 35°C threshold has been used in publications such as the IPCC Sixth Assessment Report (AR6 WGI, Fig. 12.4; IPCC, 2021).

There are limitations to our choice of indicator. Firstly, the binary threshold treats all days equally, regardless of how far they are from the 35°C cut-off. Secondly, aggregating to GAUL 2015 ADMIN1 regional boundaries could mask heat events in localised microclimates. Thirdly, this indicator solely captures temperature and excludes other components of high heat, such as humidity.

Alternative heat measures exist that include additional components of high heat. For example, the Wet Bulb Globe Temperature (WBGT) heat index estimates the level of comfort experienced during heat extremes (Brimicombe et al, 2023). It incorporates additional inputs in its model, such as wind speed and radiant temperature. However, globally available datasets covering our temporal needs are not easily accessible.

Using the 'high heat' indicator of >=30 days with a maximum temperature equal to or higher than 35 °C, we find that 33.5% of all regions–year observations globally met the heat-exposure threshold. The regions classified as 'high heat' in the latest year with MPI data can be seen in Figure 2.

Figure 2. Heat exposure by subnational region. Hazard data corresponds to the most recent MPI survey year for each region.

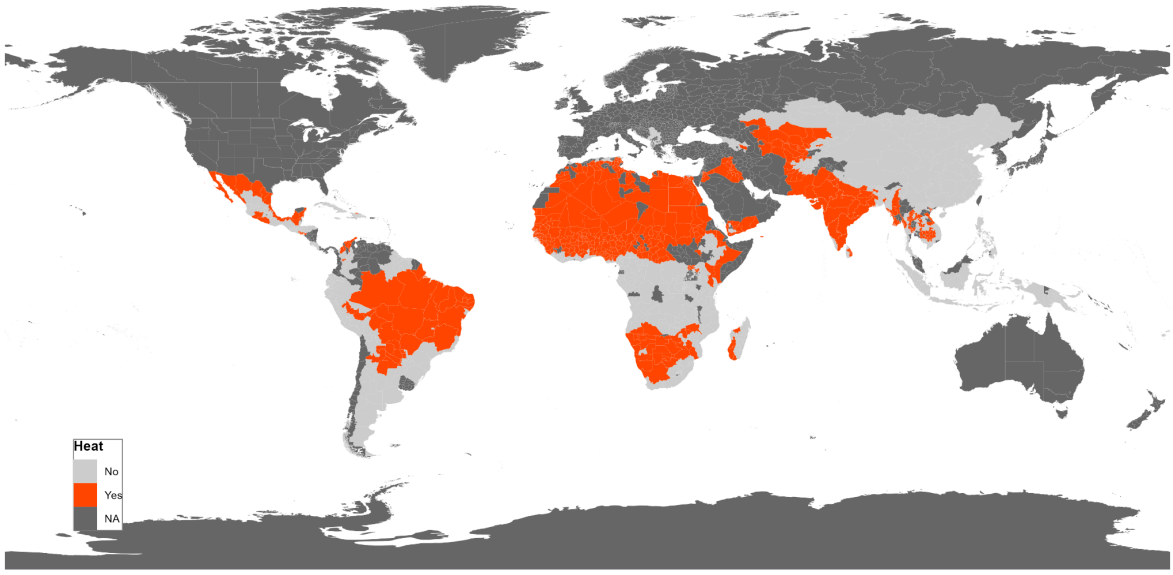

Source: Authors' calculations using ERA5 (via World Bank Climate Change Knowledge Portal) indicator "days with Tmax >= 35 °C" and GAUL 2015 ADM1; matched to Global MPI 2025 region-year.

3.2.3 Flood Measurement

The indicator used for floods comes from the Emergency Events Database (EM-DAT). EM-DAT records data on natural disasters from various sources, such as UN agencies, NGOs, and press agencies (EM-DAT, 2025). In EM-DAT, a flood is classified as a hydrological disaster. Disasters are recorded in the dataset if they meet at least one of the following criteria: (i) ten or more people died; (ii) one hundred or more people were affected (injured or left homeless); (iii) a state of emergency was declared; or (iv) there was a call for international assistance. An implication of this definition is that our analysis is limited to large-scale flood events that satisfy at least one of these criteria. Small-scale (but potentially impactful) floods are excluded.

Alternative datasets that could be used for the flood indicator use hazard-based definitions rather than impact thresholds. For example, satellite-based metrics such as the Global Flood Database (Tellman et al., 2021) and the Dartmouth Flood Observatory (Kettner et al, 2021) identify floods using physical characteristics such as the size and duration of the flood. This approach can capture floods that are not captured by datasets that use impact thresholds, such as EM-DAT. However, as we are interested in the human consequences of natural disasters, the choice to use EM-DAT is motivated by its explicit use of human impact criteria to classify floods.

To conduct the analysis, we construct a binary indicator for each region-year. The indicator is assigned a value of one if there is at least one flood within that region in the reference year. The reason for using a binary indicator – rather than examining cumulative floods or the intensity of

floods – is that a simple binary indicator allows for better data completeness, as not all floods have recorded intensity. In addition, there is a reduced risk of bias associated with inconsistent intensity reporting by different sources.

However, there are limitations to using the EM-DAT dataset for floods (Jones et al, 2022). Firstly, the analysis cannot distinguish between the intensity of different floods. While each flood event must satisfy the qualifying flood definition noted above, there is still a large range in both the coverage and time duration of the flood. Moreover, floods are often localised, as in a region marked as 'flooded' in a given year, there may be people unaffected by the flood because they live in an unaffected part of their region. Furthermore, these possibilities are not uniform across subnational regions: the possibility of over-reporting could be sharply higher in the largest or most populous regions. Finally, there is a possibility that reporting bias affects the underlying dataset. Countries with less capacity to report natural disasters and the populations affected or call for international assistance - due to a lack of an effective reporting standard or limited media presence - may experience an undercount of floods. This could bias the results if the countries with less state capacity and less media presence are also likely to be relatively poor.

Despite these caveats, EM-DAT stood out as a measure of flood climatic hazard due to its strong academic and policy reputation. It is widely used across academia and policy, such as at organisations including the United Nations (Cuthbertson et al, 2021). Moreover, the temporal and spatial coverage of EM-DAT make it suited for comparative analysis with the regional MPI data.

Using EM-DAT flood data, 13.31% of all region–year observations globally experienced at least one qualifying flood in the reference year. Restricting to countries with MPI data, the share rises to 18.2%, indicating that floods were more common in the years and regions covered by MPI data. The highest recorded incidence was in South Asia in 2017, where 83.3% of ADM1 units experienced at least one flood event (see Figure 3).

Figure 3. Flood exposure by subnational region. Hazard data corresponds to the most recent MPI survey year for each region

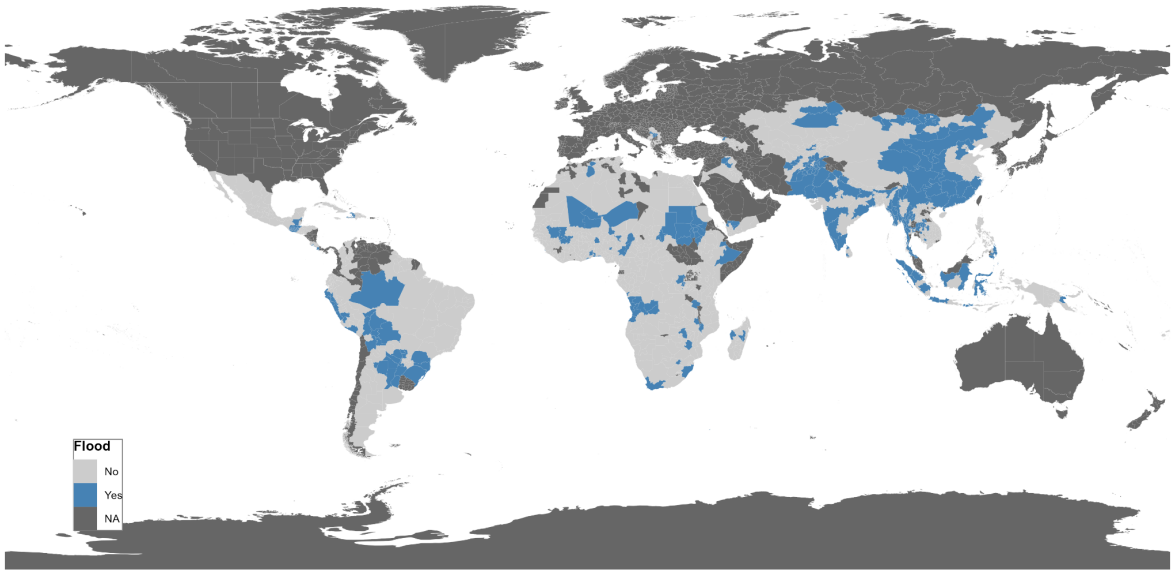

Source: Authors' calculations using EM-DAT (UCLouvain/CRED) flood events and GAUL 2015 ADM1; matched to Global MPI 2025 region-year.

3.2.4. Air pollution Measurement

The indicator used to measure air pollution is annual average surface-level PM2.5 concentration (μg/m³). PM2.5 refers to the level of fine particulate matter with a diameter < 2.5 μm suspended in the air. These particles are small enough to penetrate into the lungs and enter the bloodstream. As noted in the literature review, chronic PM2.5 exposure is linked to a variety of negative outcomes, including premature mortality and development disorders (Pozzer et al., 2023).

Our PM2.5 estimates come from the Copernicus Atmosphere Monitoring Service (CAMS) global reanalysis. CAMs provides estimates of PM2.5 from 2003 to the present at a ~0.75° native grid resolution. The PM2.5 estimates are produced by assimilating satellite retrievals and in-situ ground-based measurements into a global chemical transport model (CAMS, 2020; Eskes et al, 2024).

A region is classified as polluted if its annual mean PM2.5 exceeds 35 μg/m³. The >35 μg/m³ target comes from the WHO Interim Target 1 (IT-1). This is the first and least stringent of the four WHO PM2.5 interim targets. Following Rentschler and Leonova (2023), PM2.5 concentrations above 35 μg/m³ can be considered 'hazardous'. These targets are designed to be milestones towards reaching the WHO Air Quality Guideline of 5 μg/m³, with any concentration above this guideline considered 'unsafe' (Rentschler and Leonova, 2023).

Alternative measures of air pollution considered from the literature include health risk-based bands, which estimate the relative risk of mortality from air pollution (GBD. 2020). This type of

metric offers a nuanced measure of intensity. However, the binary variable used in our analysis would require an arbitrary cut-off along the continuous risk curve, reducing transparency. The >35 μg/m³ is chosen as our air pollution threshold because it is internationally recognised, policy relevant, and provides sufficient variation in exposure across global regions for comparative analysis.

PM2.5 was chosen as an indicator over other pollutants as it is a consistent and robust predicator of mortality (Cohen et al. 2017). For example, it is used as the measure for SDG 11.6.2, which tracks annual mean PM2.5 concentrations in cities. In addition, CAMS data is selected as the source for the PM2.5 measure for several reasons. Firstly, CAMs estimates are relatively methodologically robust. CAMs values are generated by assimilating ground values with satellite values in a chemical transport model. This allows CAMs PM2.5 estimates to avoid the data gaps that can affect satellite-only measures of PM2.5, due to cloud cover or sensor issues. In addition, CAMs is very consistent: it offers a homogenous global system over 2003-present.

However, there are limitations to using the PM2.5 data as the air pollution indicator. Firstly, the measure only captures ambient outdoor PM2.5. It does not include indoor air pollution, which remains a significant health burden in many countries as mentioned above (cf Smith et al., 2014). Furthermore, PM2.5 cannot distinguish the cause of pollution. High PM2.5 values could come from natural events, such as dust storms or volcanic eruptions, or could come from anthropogenic sources, such as vehicle emissions or industrial activity. This can make it difficult to identify effective policies to lower air pollution exclusively using a measure of PM2.5.

Using the PM2.5 > 35 μg/m³ threshold, 14.81% of region–year observations in the global panel dataset are classified as polluted. When exclusively examining regions with MPI values, the share of polluted regions rises to 21.5%. Figure 4 provides a global overview of the regions recorded as 'polluted' in the most recent year with MPI data for that region.

It is important to note a distinction between air pollution and the other three hazards examined in this analysis: high heat, droughts, and floods. While some air pollution is directly generated by human activities and linked to industrialization, some types of air pollution, and of the other climate hazards are shaped by natural variability but increasingly intensified by human-driven climate change and land-use practices. In this sense, both represent critical human-environment interactions, but through different pathways; droughts, floods and heat hazards are amplified by anthropogenic change, whereas air pollution arises directly from it. Together, they reveal how multiple human-driven processes, whether through direct emissions or climate intensification,

converge to deepen poverty and vulnerability. We present a summary of the hazards' definitions in Table 3.

Figure 4. Air Pollution exposure by subnational region. Hazard data corresponds to the most recent MPI survey year for each region

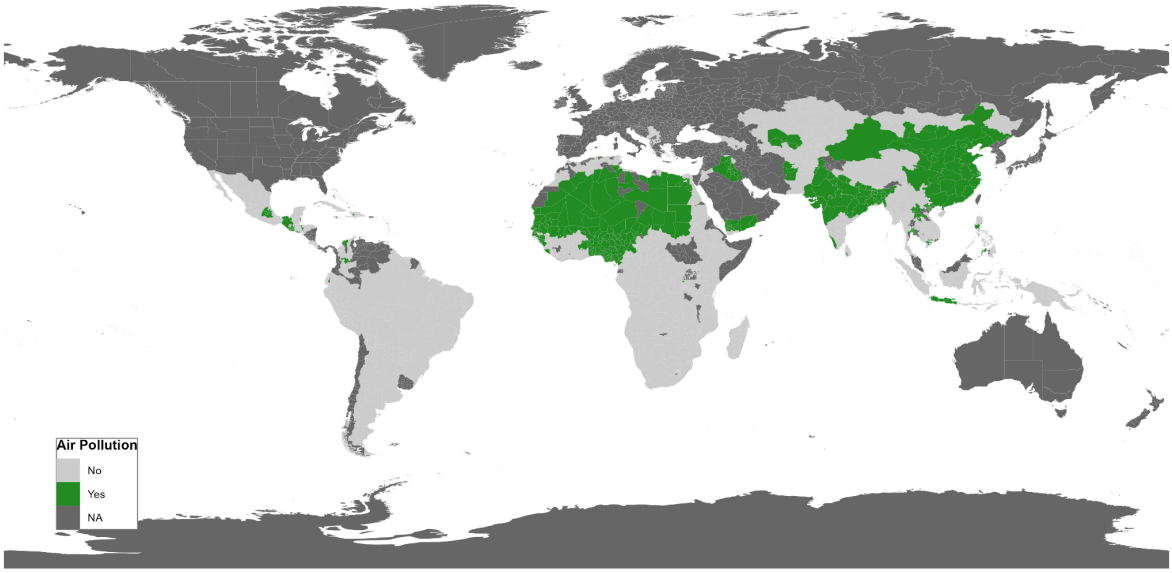

Source: Authors' calculations using CAMS global reanalysis (EAC4) $PM_{2.5}$ annual mean and GAUL 2015 ADM1; matched to Global MPI 2025 region-year.

Table 3: Environment hazards, definitions and sources

Hazard	Definition	Primary Data Source
High Heat	>= 30 days/year where daily max temperature >= 35 °C	ERA5-reanalysis, via the World Bank Climate Change Knowledge Portal
Drought	Annual mean $SPEI_{12} \leq -1$	ERA5 reanalysis
Flood	≥ 1 qualifying flood event/year (≥10 deaths, ≥100 affected, state of emergency, or international assistance)	EM-DAT (CRED, 2024)
Air Pollution ($PM_{2.5}$)	Annual mean $PM_{2.5}$ > 35 μg/m³ (WHO IT-1 threshold)	CAMS global reanalysis EAC4

Source: Authors' own compilation.

3.3 Forward-looking mapping of MPI and climate: Integrating poverty with temperature projection data

To examine whether there is a geographical overlap in the prevalence of multidimensional poverty with extreme temperature rise in the future, we integrate global MPI 2025 country- level MPI estimates with country-level average projections of daily temperatures for the time periods: 2040-59, and 2080–99, from UNDP's Human Climate Horizons (HCH) Platform. The projections are based on Representative Concentration Pathways (RCP), a set of future climate scenarios. RCPs are different "what if" storylines that describe how much greenhouse gas the world might emit in

the future and how those emissions would affect the Earth's climate. Temperature projections for two scenarios were used in this analysis: RCP 4.5 and RCP 8.5. RCP 4.5 represents a moderate scenario, in which countries achieve their current pledges to the Paris Agreement and global greenhouse gas emissions peak around mid-century, and RCP 8.5 represents a high emission scenario in which global emissions continue to climb to high levels for the rest of the century. To derive temperature projections for these scenarios, HCH uses information from CMIP5 (Coupled Model Intercomparison Project Phase 5), a major research effort involving scientists from around the world running sophisticated climate models simulating Earth's climate system and providing a wide range of data (including temperature, rainfall, wind patterns, ocean circulation etc.), to understand how the climate might respond to different greenhouse gas levels. The gridded temperature projections were aggregated to regional estimates by first transforming the daily minimum, average, or maximum temperature at the grid scale, then aggregating to regions using a weighted average. The average annual number of high heat days, or days above the threshold of 35 Celsius for the two timeframes, 2040-59, and 2080-99, were then calculated for each climate scenario for the regions. We estimate the projected increase in the number of high heat days by subtracting the projected number of days from the historical average for the timeframe 1986-2005 for each sampled country.

By merging country-level temperature projection information with the MPI data, we are able to assess whether countries that currently experience higher levels of multidimensional poverty are expected to experience the highest increases in the number of high heat days in the future.

3.4 Methodological Limitations

It is important to acknowledge limitations to the approach. First, aligning environmental data for a single year to a single MPI reference year provides only a snapshot in time. Climate hazards like droughts and floods are seasonal and can vary significantly over short periods (as can poverty), while heat and air pollution can change daily or even hourly. As a result, although our standards for hazards sought to identify serious conditions (floods, injuries, high levels of PM2.5) they may still overlook important temporal patterns or variations in intensity and thus mis-state the full extent of people's vulnerability. To mitigate this issue, measures of the hazards were chosen to represent as broad a range of as the data allowed, such as annual average air pollution levels.

Second, combining data at the subnational level (Admin1 GAUL regions) requires spatial averaging. This can hide important differences within regions, because not all poor individuals may be equally exposed to or affected by climate hazards. Finer-tuned, localized hotspots where poverty and environmental risks overlap may be masked when data are aggregated at larger scales.

To mitigate the issue that the high levels in the environmental hazard are driven by localised outlier values, we winsorized drought and air pollution data at the 95th percentile.

Third, subnational administrative areas differ widely in size across countries. This variation affects the accuracy of spatial overlays and can obscure local climate risks. A severe event in a small area might appear insignificant when averaged across a much larger administrative unit. For example, severe flooding along the Solimões River in 2015 had devastating effects across isolated towns and indigenous communities in the states of Acre and Amazonas in the Brazilian Amazon (see Silva Araújo et al, 2022). However, because these states span over 152 thousand people and 1.5 million square kilometers, respectively, such localized disasters appear diluted in regional analyses, leading to an imperfect estimation of the link between flooding and multidimensional poverty.

Finally, a one-year cross-section of poverty cannot capture dynamic processes of adaptation, resilience, or mobility, and the observed correlations may also reflect other structural determinants, such as governance quality or historical inequalities. As a result, these analyses should be interpreted as descriptive rather than causal. Still, they represent a valuable step in integrating climate and poverty research, offering both a diagnostic tool for understanding the geography of deprivation and a foundation for more longitudinal or causal studies

Despite these challenges, which mainly reflect data scarcity, our analysis represents an important step toward understanding how environmental stressors intersect with multidimensional poverty on a global scale. These limitations also highlight the need for ongoing improvements in data quality and more localized assessments to fully capture the complexity of this relationship. Thus our study contributes novel evidence by bringing together three analytical angles that have rarely been combined before: a subnational perspective to understand the relationship between climate hazards and poverty, a multidimensional approach to the latter, and a large-scale, cross-country scope. This unique combination allows for a richer understanding of spatial and compositional inequalities in vulnerability to environmental stressors, offering a new empirical basis for both research and policy discussion.

4. Results

Overall, 59.1% of the sampled 1716 sub-national regions with climate hazard data experienced at least one of the four climate hazards in the year in which poverty was measured. These exposed areas are home to around 887 million multidimensionally poor people, which covers 78.8% of the 1.1 billion total global poor. Among the four climate hazards, the largest number of poor people live in areas exposed to high heat (608 million), followed by air pollution (577 million) and floods

(465 million). Around 207 million poor people live in sub-national areas exposed to droughts (Table 4).

Table 4: Number and percentage of multidimensionally poor population exposed to climate hazards, by region and income groups

	High heat	Drought	Flood	Air pollution	Any of the four hazards	Two or more hazards	Three or more hazards	All four hazards
	Number of poor people (million); Incidence of MPI in that region/group							
World	608; 54.0%	207; 18.4%	465; 41.3%	577; 51.3%	887; 78.8%	651; 57.8%	309; 27.4%	11; 1.0%
Region								
Sub-Saharan Africa	229; 41.0%	147; 26.3%	83; 14.8%	158; 28.3%	344; 61.7%	193; 34.6%	72; 12.9%	6; 1.2%
South Asia	308; 80.4%	28; 7.2%	291; 75.8%	333; 86.7%	380; 99.1%	351; 91.6%	226; 59.0%	2; 0.5%
Latin America and the Caribbean	11;36.1%	9; 27.4%	11; 34.9%	5; 17.6%	26; 84.4%	10; 31.1%	0; 0.5%	-
Europe and Central Asia	0.6; 37.8%	0.7; 41.6%	0.2; 11.9%	0.2; 10.9%	1.0; 60.2%	1; 33.7%	0; 8.2%	-
East Asia and the Pacific	17; 16.8%	11; 11.1%	58; 56.8%	57; 55.8%	87; 84.8%	57; 55.4%	0; 0.1%	-
Arab States	42; 85.0%	12; 24.7%	23; 45.6%	25; 49.5%	48; 97.6%	40; 80.5%	10; 20.7%	3; 6%
Income group								
Low income	144; 35.8%	97; 24.1%	92; 23.0%	72; 18.0%	246; 61.3%	123; 30.7%	31; 7.7%	5; 1.3%
Lower middle income	446; 71.7%	89; 14.4%	325; 52.1%	441; 70.9%	548; 88.0%	470; 75.6%	277; 44.4%	6; 1%
Upper middle income	18;18%	21; 20.6%	48; 47.4%	64; 63.0%	93; 91.1%	58; 56.5%	1; 1.3%	-

Source: Authors' calculations based on Global MPI 2025 aggregates by GAUL 2015 ADM1 overlaid with hazard exposure flags (ERA5/CCKP, ERA5-Drought SPEI, EM-DAT, CAMS).

Many poor individuals face overlapping exposure; 11 million multidimensionally poor people live in areas experiencing all four hazards of high heat, drought, flood, and air pollution. Around 57.8% of the global poor, or 651 million poor people live in areas exposed to at least two or more climate hazards and 27.4% (309 million) are exposed to three or more hazards.

4.1 Overlaps by Region

As we show in Figure 5, Sub-Saharan Africa and South Asia report the largest number of poor people residing in places affected by the examined climate hazards. In Sub-Saharan Africa, 61.7% of the poor population, or 344 million poor, live in areas experiencing at least one climate hazard. In South Asia, a slightly higher number, 380 million poor people live in areas exposed to the hazards. These however constitute an overriding 99.1% of the total multidimensionally poor people in South Asia (Table 1). Among the types of hazards, air pollution affects the largest number of poor people in South Asia; around 333 million, or 86.7% of the poor in the region live in places exposed to PM2.5 levels higher than 35 μg/m³. This is followed by high heat which affects 80.4% of poor people (308 million).

While other world regions have smaller populations living in multidimensional poverty, they still face considerable environmental risks. In East Asia and the Pacific, 56.8% of the poor are exposed to floods and 55.8% to air pollution. In the Arab States, 85.0% of the poor face high heat (42 million). Additionally, poor people in the Arab States also face substantial exposure to floods (45.6% or 23 million poor) and air pollution (49.5% or 25 million poor). Latin America and the Caribbean show similar exposure to all climate hazards, with about a third of the poor facing heat stress, floods, and drought (36.1%, 34.9%, and 27.4% of the poor population respectively). Europe and Central Asia have comparatively lower poverty levels, yet a notable portion of the poor population is exposed to environmental hazards such as drought (41% or 0.7 million poor) and heat (37% or 0.6 million poor).

Figure 5: Number of poor populations living in areas exposed to concurrent hazards, by region and income groups.

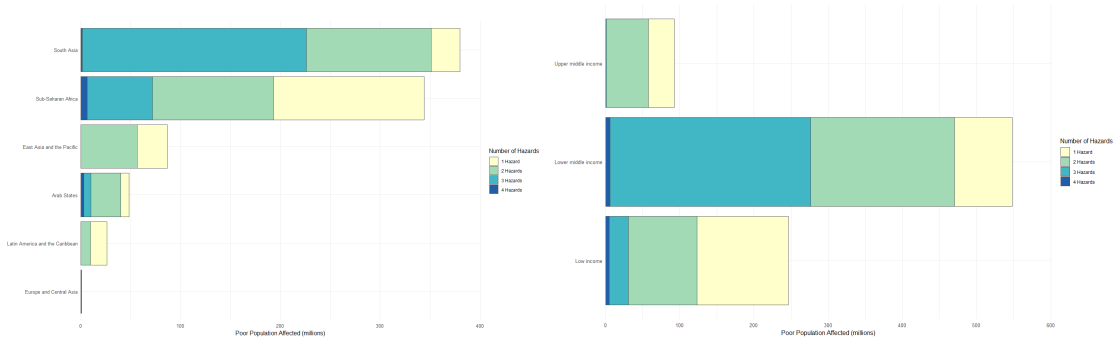

Source: Authors' calculations from overlays of Global MPI 2025 with ERA5/CCKP (>=35 °C days), ERA5-Drought SPEI, EM-DAT floods, and CAMS $PM_{2.5}$.

4.2 Trends by Income Groups

Environmental hazard exposure varies significantly across country income groups. In lower-middle income countries, 88.0% of the poor, or 548 million individuals, live in areas exposed to at least one of the four environmental hazards. Of these, the majority are affected by high heat (71.7% or 446 million), followed by floods (52.1% or 325 million), and air pollution (70.9% or 441 million. Over 470 million of these individuals are simultaneously exposed to multiple and compounding risks, a level of overlapping vulnerability not seen in other income groups (Figure 2). Low-income countries also face high exposure to certain hazards, especially heat, which affects approximately 35.8% (144 million) of poor people. A similar number of people in low-income countries are exposed to drought and floods - 97 million or 24.1% of the poor for drought and 92 million or 23.0% for floods. However, the incidence of overlapping exposure, where individuals are simultaneously affected by multiple hazards, is considerably lower than in lower-middle-income countries.

In contrast, upper-middle-income countries show markedly lower levels of exposure among the poor. Fewer than 91.1% (93 million) of poor people in these countries live in areas facing climate-related risks, and most are exposed to just one or two hazards. Nonetheless, air pollution and flooding remain significant, affecting 63% (64 million) and 47.4% (48 million) of the poor population, respectively.

4.3 Trends in Types of Deprivation

Table 5 presents the number of multidimensionally poor people deprived in each of the MPI indicators, by exposure and non-exposure to at least one type of climate hazard. Among poor populations living in sub-national areas exposed to at least one climate hazard, the largest numbers are deprived in cooking fuel, housing, and sanitation, each affecting more than 600 million people. Large numbers also face deprivations in nutrition (506 million), years of schooling (461 million), and school attendance (384 million). These findings highlight that deficits in basic services and living standards affect the greatest share of poor people exposed to climate risks, alongside persistent shortfalls in health and education. For those living in areas not exposed to any of the four hazards, deprivation patterns follow similar trends but at much smaller scales. The largest deprivations remain in cooking fuel (229 million), housing (208 million), and sanitation (196 million), with electricity (192 million) close behind.

Across world regions, deprivation profiles vary. Among those living in areas exposed to climate hazards in South Asia, the highest deprivations are in housing (315 million), cooking fuel (281 million), and nutrition (270 million). In Sub-Saharan Africa, deprivation in cooking fuel is most

widespread, affecting 332 million poor people, followed by sanitation (286 million), electricity (279 million), and housing (278 million). While absolute numbers of deprived poor are larger in South Asia, the proportion of the poor population experiencing deprivations is consistently higher in Sub-Saharan Africa.

Table 5: Number of multidimensionally poor people deprived in different MPI indicators.

	Global (Number of poor and deprived; in millions)		By regions (Number of poor and deprived in areas exposed to at least one climate hazard; in millions)					
MPI Indicator	**Sub-national area exposed to any climate hazard**	**Sub-national area unexposed to any climate hazard**	**Arab States**	**East Asia and the Pacific**	**Europe and Central Asia**	**Latin America and the Caribbean**	**South Asia**	**Sub-Saharan Africa**
Assets	366.7	151.1	22.5	23.1	0.0	7.2	138.4	175.5
Child Mortality	115.9	21.4	5.8	5.8	0.8	5.7	40.8	57.1
Cooking Fuel	726.3	229.1	31.0	66.5	0.2	15.7	280.5	332.5
Electricity	379.4	192.2	22.6	16.7	0.0	6.3	55.1	278.7
Housing	654.1	208.1	24.5	23.3	0.3	13.0	315.1	277.9
Nutrition	506.3	116.6	31.1	57.0	0.3	11.5	270.3	136.1
Sanitation	616.9	196.5	31.2	33.8	0.1	15.8	249.8	286.2
School Attendance	383.5	94.6	25.0	33.3	0.2	5.3	144.8	174.8
Water	355.1	153.4	25.0	36.0	0.2	10.2	70.3	213.4
Years of Schooling	461.4	107.2	23.5	46.6	0.0	11.4	204.0	175.8
Total Poor Population	886.6	239.2	48.5	86.8	1.0	26.4	380.1	343.9

Source: Authors' calculations based on Global MPI 2025 aggregates by GAUL 2015 ADM1 overlaid with hazard exposure flags (ERA5/CCKP, ERA5-Drought SPEI, EM-DAT, CAMS).

4.4 Trends by Future Temperature projections

Countries with higher levels of multidimensional poverty are expected to face larger increases in the average number of days with high heat (maximum temperatures above 35°C). As we show in Figure 6, under a moderate emissions scenario, countries in the highest poverty quartile are projected to experience an increase of 28 additional high heat days annually by 2040–2059; by 2080-99 the number increases to 39. Under a high emissions scenario, countries in the highest poverty quartile are projected to experience 37 additional high-heat days annually by 2040–2059, and rising to 92 days by 2080–2099. In contrast, countries in the lowest poverty quartile are

expected to see a relatively smaller increase, ranging from 24 to 62 additional high-heat days per year by the end of the century.

Figure 6: Average increase in number of high heat days across countries, by MPI quartiles

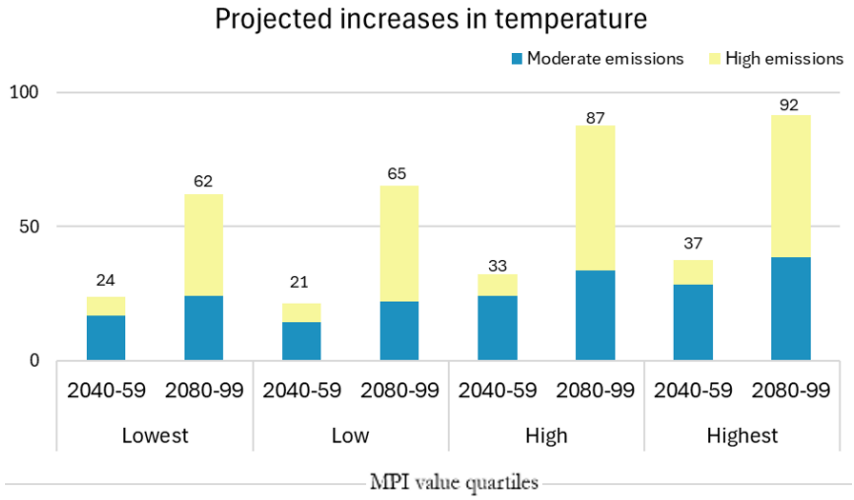

Source: Authors' calculations using UNDP Human Climate Horizons (CMIP5; RCP4.5/RCP8.5) country-level projections merged with Global MPI 2025.

5. Discussion

The results underscore three broad insights that should shape how researchers and policymakers think about the climate–poverty nexus.

First, subnational analyses can illuminate heterogeneity that national averages overlook. Many countries display large internal variation in both multidimensional poverty and climate hazard exposure. For each hazard, roughly half of all countries display internal diversity in exposure patterns: 46 countries for drought, 49 for floods, 54 for heat, and 40 for air pollution. National statistics, therefore, risk underestimating the number of people simultaneously facing deprivation and environmental risk. Although insightful, our results only partially gauge the extent of this problem due to data limitations. The existence of concentrated pockets including urban informal settlements, marginalized rural districts, and particular ecological zones highlights the necessity of geographically targeted policies that respond to local risk profiles rather than one-size-fits-all national programs.

Second, overlapping and compounding hazards are common globally. Our estimates show that around 651 million poor people live in areas exposed to at least two climate hazards in the same year, and 309 million are exposed to three or more. The prevalence of multi-hazard exposure, whereby populations face multiple hazards in the same place and year, amplifies vulnerability to non-monetary deprivations in ways that single-hazard analyses cannot capture. Multi-hazard

exposure intensifies pressures on livelihoods, health systems, infrastructure, and household budgets, making recovery slower and more costly and increasing the likelihood of persistent poverty traps. The concentration of multi-hazard burdens in regions such as South Asia and sub-Saharan Africa indicates where integrated adaptation and social protection efforts could deliver quite important results to improve true sustainable development.

Third, the distributional dimension of future heat risk is stark. Country-level projections indicate that places with higher current multidimensional poverty are expected to experience larger increases in extreme heat days under high emissions pathways. This asymmetric exposure compounds existing inequalities: populations that already lack access to cooling, reliable health care, and resilient livelihoods are likely to be those most affected by rising heat burdens. Early investment in heat-sensitive sectors—public health, schooling, informal market protections, and labor regulations—therefore represents a high-priority, equity-focused adaptation agenda.

Notwithstanding these conclusions, important methodological caveats must be considered and properly addressed in subsequent research. The analysis relies on spatial aggregation to administrative units, which can obscure within-unit heterogeneity and dilute localized extreme events. The cross-sectional matching of hazard data to single-year MPI observations provides a descriptive snapshot but cannot, in itself, establish causal pathways or capture temporal dynamics of adaptation and mobility. Also, hazard measures differ in nature and coverage—impact-based flood registers versus reanalysis products for heat and drought or modeled PM2.5 fields for air pollution—introducing measurement asymmetries that the analysis seeks to document and to which results should be interpreted accordingly.

Taken together, these results call for a careful blend of precision and pragmatism: More granular, frequent data collection on poverty and flooding, and causal research on mechanisms, alongside immediate, place-based policy responses where high poverty and high hazard exposure coincide.

At the same time, this study is pioneering in several ways: it is the first to have overlaid multidimensional poverty with climate hazards at a global scale and with subnational detail. This work could be extended in a number of beneficial ways. First, additional definitions of these four variables and additional standards of 'hazardous exposure' could be implemented. Second, additional climate hazards could be included – such as fires, cyclones, salination, forest loss, loss of biodiversity, earthquakes – as could alternative hazards with subnational data, such as conflicts and food security. Third, by analysing temporal dynamics: how the trends in poverty and climate change over time.Finally, mixed methods analyses to include historical, political, community-based and institutional layers, for example, will greatly expand the depth of understanding generated.

The spatially explicit patterns revealed in our assessment point toward a set of complementary policy priorities that can help reduce present vulnerabilities to non-monetary hardships while building longer-term resilience to adverse climate conditions.

6. Conclusion

This paper provides a globally comparable, subnational assessment of the intersection between climate hazards and multidimensional poverty. The results suggest that overlap is endemic. An estimated 887 million multidimensionally poor people live in regions exposed to at least one hazard in the same year. Almost 60% of multidimensionally poor people (651 million) experience overlapping exposure to two or more hazards, and 11 million face all four hazards simultaneously. There is clear regional concentration in the number of poor people exposed to hazards. For instance, South Asia and Sub-Saharan Africa alone account for more than an estimated 700 million poor people exposed to environmental hazards. Looking ahead, projections suggest that countries with the highest poverty rates today are likely to suffer the greatest increases in exposure to future extreme heat.

These findings provide three key insights. First, subnational analyses can provide a means of identifying uneven patterns of poverty and environmental hazard exposure within countries. Second, exposure to multiple hazards simultaneously is common globally. Third, future trends in hazards suggest that the countries with the least adaptive capacity to future risks are the most likely to experience intensifying hazards. Taken together, the results suggest that poverty and climate hazards are not parallel challenges but mutually reinforcing phenomena.

References

Alderman, H., Hoddinott, J., and Kinsey, B. (2006). Long-term consequences of early childhood malnutrition. The American Journal of Clinical Nutrition, 83(5), 1191–1195.

Alkire, S., and Santos, M. E. (2014). Measuring acute poverty in the developing world: Robustness and scope of the multidimensional poverty index. World Development, 59, 251-274.

Alkire, S., Kanagaratnam, U., Nogales, R., and Suppa, N. (2022). Revising the global multidimensional poverty index: Empirical insights and robustness. Review of Income and Wealth, 68, S347-S384.

Allen, M. J., Vecellio, D. J., and Hoffman, J. S. (2025). Evaluating the relationship between heat-related illness and cooling center location in Virginia. Natural Hazards, 121(4), 4293-4308.

Amoako, C., and Frimpong Boamah, E. (2015). The three-dimensional causes of flooding in Accra, Ghana. International Journal of Urban Sustainable Development, 7(1), 109-129.

Anderson, G. B., and Bell, M. L. (2011). Heat waves in the United States: mortality risk during heat waves and effect modification by heat wave characteristics in 43 US communities. Environmental health perspectives, 119(2), 210-218.

Arceo-Gomez, E. O., and López-Feldman, A. (2024). Extreme temperatures and school performance of the poor: Evidence from Mexico. Economics Letters, 238, 111700.

Azzarri, C., and Signorelli, S. (2020). Climate and poverty in Africa South of the Sahara. World development, 125, 104691

Barrett, C. B., and Carter, M. R. (2006). The economics of poverty traps and persistent poverty: An asset-based approach. Journal of Development Studies, 49(12), 1700–1715.

Barrett, C. B., and Carter, M. R. (2013). The economics of poverty traps and persistent poverty: Empirical and policy implications. The Journal of Development Studies, 49(7), 976-990.

Berger, S.E., Ordway, M.R., Schoneveld, E., Lucchini, M., Thakur, S., Anders, T., Natale, L. and Barnett, N. (2023). The impact of extreme summer temperatures in the United Kingdom on infant sleep: Implications for learning and development. Scientific reports, 13(1), 10061.

Blom, S., et al. (2022). "Heat and child nutrition in Africa." Journal of Environmental Economics and Management, 113, 102647. → Direct evidence that higher temperatures worsen child malnutrition.

Brimicombe, C., Lo, C.H.B., Pappenberger, F., Di Napoli, C., Maciel, P., Quintino, T., Cornforth, R. and Cloke, H.L. (2023). Wet bulb globe temperature: Indicating extreme heat risk on a global grid. GeoHealth, 7(2), p.e2022GH000701.

Byers, E., Gidden, M., Leclère, D., Balkovic, J., Burek, P., Ebi, K., ... and Riahi, K. (2018). Global exposure and vulnerability to multi-sector development and climate change hotspots. Environmental Research Letters, 13(5), 055012.

Cohen, A.J., Brauer, M., Burnett, R., Anderson, H.R., Frostad, J., Estep, K., Balakrishnan, K., Brunekreef, B., Dandona, L., Dandona, R. and Feigin, V., 2017. Estimates and 25-year trends of the global burden of disease attributable to ambient air pollution: an analysis of data from the Global Burden of Diseases Study 2015. The lancet, 389(10082), pp.1907–1918.

Copernicus Atmosphere Monitoring Service (CAMS). (2020). CAMS global reanalysis (EAC4) [Data set]. Copernicus Atmosphere Monitoring Service (CAMS) Atmosphere Data Store.

CRED (2020). The Human Cost of Disasters 2000–2019. Centre for Research on the Epidemiology of Disasters.

Cuthbertson, J., Archer, F., Robertson, A., and Rodriguez-Llanes, J. M. (2021). Improving disaster data systems to inform disaster risk reduction and resilience building in Australia: a comparison of databases. Prehospital and disaster medicine, 36(5), 511–518.

Daniel, V. E., Florax, R. J., and Rietveld, P. (2009). Flooding risk and housing values: An economic assessment of environmental hazard. Ecological Economics, 69(2), 355–365.

Dell, M., Jones, B. F., and Olken, B. A. (2014). What do we learn from the weather? The new climate-economy literature. Journal of Economic Literature, 52(3), 740–798.

Dercon, S., and Porter, C. (2014). Live Aid revisited: Long-term impacts of the 1984 Ethiopian famine on child stunting. Journal of the European Economics Association, 108, 1–18.

Dimitrova, A., et al. (2024). Temperature-related neonatal deaths attributable to climate change in 29 low- and middle-income countries. Nature Communications, 15, 49890.

Doan, M. K., Hill, R., Hallegatte, S., et al. (2023). Counting People Exposed to, Vulnerable to, or at High Risk from Climate Shocks—A Methodology (No. 10619). The World Bank.

Douglas, I., Alam, K., Maghenda, M., Mcdonnell, Y., McLean, L., and Campbell, J. (2008). Unjust waters: climate change, flooding and the urban poor in Africa. Environment and urbanization, 20(1), 187–205.

Drechsler, M. B. S., and Soer, W. (2016). Early warning, early action: the use of predictive tools in drought response through Ethiopia's productive safety net programme. World Bank Policy Research Working Paper, (7716).

Emergency Events Database (EM-DAT). (2025). UCLouvain/CRED, accessed on 2025-03-01.

Eskes, H., Tsikerdekis, A., Ades, M., Alexe, M., Benedictow, A.C., Bennouna, Y., Blake, L., Bouarar, I., Chabrillat, S., Engelen, R. and Errera, Q., 2024. Evaluation of the copernicus atmosphere monitoring service cy48r1 upgrade of june 2023. Atmospheric Chemistry and Physics, 24(16), pp.9475-9514.

Franceschini, G., Khan, A., Moretti, L., Nyabuti, K., Asif, M., Bezuidenhoudt, E., and Morteo, K. (2025). The Global Administrative Unit Layers (GAUL) 2024.

GBD 2019 Risk Factors Collaborators (2020). Global burden of 87 risk factors in 204 countries and territories, 1990-2019: a systematic analysis for the Global Burden of Disease Study 2019. Lancet (London, England), 396(10258), 1223–1249.

Hallegatte, S., Bangalore, M., Bonzanigo, L., Fay, M., Narloch, U., Rozenberg, J., and Vogt-Schilb, A. (2014). Climate change and poverty--an analytical framework. World Bank Policy Research Working Paper, (7126).

Hallegatte, S., Vogt-Schilb, A., Rozenberg, J., Bangalore, M., and Beaudet, C. (2020). From poverty to disaster and back: A review of the literature. Economics of Disasters and Climate Change, 4, 223–247.

Hasan, F., Marsia, S., Patel, K., Agrawal, P., and Razzak, J. A. (2021). Effective community-based interventions for the prevention and management of heat-related illnesses: a scoping review. International journal of environmental research and public health, 18(16), 8362.

Heal, G., and Park, J. (2016). Reflections—temperature stress and the direct impact of climate change: a review of an emerging literature. Review of Environmental Economics and Policy.

Hersbach, H., Bell, B., Berrisford, P., Hirahara, S., Horányi, A., Muñoz-Sabater, J., ... and Thépaut, J. N. (2020). The ERA5 global reanalysis. Quarterly journal of the royal meteorological society, 146(730), 1999-2049.

Hoddinott, J. (2006). Shocks and their consequences: The implications for food security. Food Policy, 31(5), 373–382.

Hill, R., Gorgulu, N., Brunckhorst, B., Nguyen, M., Hallegatte, S., and Naikal, E. (2025). One-fifth of the world's population at high risk from climate-related hazards.

Hossain, B., Sarker, M. N. I., Shi, G., and Sohel, M. S. (2023). Household vulnerability and resilience to natural disasters in Pakistan: A systematic literature review. Disaster, displacement and resilient livelihoods: Perspectives from South Asia, 35-53.

ILO (2024). World Social Protection Report 2024–26: Universal Social Protection for Climate Action. International Labour Organization.

Intergovernmental Panel on Climate Change (IPCC). (2021). Climate change 2021: The physical science basis. Contribution of Working Group I to the Sixth Assessment Report of the Intergovernmental Panel on Climate Change (V. Masson-Delmotte, P. Zhai, A. Pirani, S. L. Connors, C. Péan, S. Berger, N. Caud, Y. Chen, L. Goldfarb, M. I. Gomis, M. Huang, K. Leitzell, E. Lonnoy, J. B. R. Matthews, T. K. Maycock, T. Waterfield, O. Yelekçi, R. Yu, and B. Zhou, Eds.). Cambridge University Press.

IPCC AR6 WGII (2022). Climate Change 2022: Impacts, Adaptation and Vulnerability.

Jones, R. L., Guha-Sapir, D., and Tubeuf, S. (2022). Human and economic impacts of natural disasters: can we trust the global data? Scientific data, 9(1), 572.

Lelieveld, J., Evans, J.S., Fnais, M., Giannadaki, D. and Pozzer, A., 2015. The contribution of outdoor air pollution sources to premature mortality on a global scale. Nature, 525(7569), pp.367–371.

Jafino, B. A., Hallegatte, S., Rozenberg, J., and Walsh, B. (2023). Revised estimates of the impact of climate change on extreme poverty by 2030. World Bank Policy Research Working Paper, (8955).

Jensen, R. (2000). Agricultural volatility and investments in children's human capital. American Economic Review, 90(2), 395–398.

Kettner, A.J., Brakenridge, G.R., Schumann, G.J. and Shen, X., 2021. DFO—flood observatory. In Earth observation for flood applications (pp. 147–164). Elsevier.

Lelieveld, J., Evans, J. S., Fnais, M., Giannadaki, D., and Pozzer, A. (2015). The contribution of outdoor air pollution sources to premature mortality on a global scale. Nature, 525(7569), 367–371.

Lieber, M., Chin-Hong, P., Kelly, K., Dandu, M. and Weiser, S.D., 2022. A systematic review and meta-analysis assessing the impact of droughts, flooding, and climate variability on malnutrition. Global Public Health, 17(1), pp. 68–82.

McFarlane, C. (2008). Sanitation in Mumbai's informal settlements: State,'slum', and infrastructure. Environment and planning A, 40(1), 88–107.

McKee, T. B., Doesken, N. J., and Kleist, J. (1993). The relationship of drought frequency and duration to time scales. In Proceedings of the 8th Conference on Applied Climatology (Vol. 17, No. 22, pp. 179–183).

Mishra, A. K., and Singh, V. P. (2010). A review of drought concepts. Journal of hydrology, 391(1-2), 202–216.

Modi, R. (2009). Resettlement and rehabilitation in urban centres. Economic and Political Weekly, 20–22.

Mora, C., Dousset, B., Caldwell, I.R., Powell, F.E., Geronimo, R.C., Bielecki, C.R., Counsell, C.W., Dietrich, B.S., Johnston, E.T., Louis, L.V. and Lucas, M.P. (2017). Global risk of deadly heat. Nature climate change, 7(7), pp.501-506.

Moyer, J. D., Pirzadeh, A., Irfan, M., Solórzano, J., Stone, B., Xiong, Y., Hanna, T., and Hughes, B. B. (2023). How many people will live in poverty because of climate change? A macro-level projection analysis to 2070. Climatic Change, 176(10), 137.

Oxford Poverty and Human Development Initiative and United Nations Development Programme (2025) The Global Multidimensional Poverty Index 2025. *Overlapping Hardships: Poverty and Climate Hazards*. New York: UNDP.

Pastor, M., Sadd, J. and Hipp, J., 2001. Which came first? Toxic facilities, minority move-in, and environmental justice. Journal of urban affairs, 23(1), pp.1-21.

Pérez-Peña, M. D. C., Jiménez-García, M., Ruiz-Chico, J., and Peña-Sánchez, A. R. (2021). Analysis of research on the SDGs: the relationship between climate change, poverty and inequality. Applied Sciences, 11(19), 8947.

Pozzer, A., Anenberg, S. C., Dey, S., Haines, A., Lelieveld, J., and Chowdhury, S. (2023). Mortality attributable to ambient air pollution: A review of global estimates. GeoHealth, 7(1), e2022GH000711.

Rees, N., 2016. Clear the air for children: the impact of air pollution on children. New York: UNICEF Division of Data. Research and Policy.

Rentschler, J., Salhab, M., and Jafino, B. A. (2022). Flood exposure and poverty in 188 countries. Nature Communications, 13(1), 3527.

Rentschler, J., and Leonova, N. (2023). Global air pollution exposure and poverty. Nature communications, 14(1), 4432.

Silva Araújo, R., Ohara, M., Miyamoto, M., and Takeuchi, K. (2022). Flood impact on income inequality in the Itapocu River basin, Brazil. Journal of Flood Risk Management, 15(3), e12805.

Smith, K. R., Mehta, S., and Feuz, M. (2002). The global burden of disease from indoor air pollution: results from comparative risk assessment. Indoor Air, 10-19.

Sudarshan, A., and Tewari, M. (2014). The economic impacts of temperature on industrial productivity: Evidence from indian manufacturing (No. 278). Working paper.

Tate, E., Rufat, S., Rahman, M. A., and Hoover, S. (2025). Profiles of social vulnerability for flood risk reduction. International Journal of Disaster Risk Reduction, 118, 105250.

Tellman, B., Sullivan, J.A., Kuhn, C., Kettner, A.J., Doyle, C.S., Brakenridge, G.R., Erickson, T.A. and Slayback, D.A., 2021. Satellite imaging reveals increased proportion of population exposed to floods. Nature, 596(7870), pp.80-86.

Tonmoy, F. N., El-Zein, A., and Hinkel, J. (2014). Assessment of vulnerability to climate change using indicators: a meta-analysis of the literature. Wiley Interdisciplinary Reviews: Climate Change, 5(6), 775-792.

Satterthwaite, D., Archer, D., Colenbrander, S., Dodman, D., Hardoy, J., Mitlin, D. and Patel, S., 2020. Building resilience to climate change in informal settlements. One earth, 2(2), pp.143-156.

Seposo, X., Celis-Seposo, A. K., Uttajug, A., Tajudin, M. A. B. A., and Ueda, K. (2025). Impact of prenatal drought exposures on under-5 childhood stunting in 32 low-and-middle-income countries: a global analysis using demographic and health survey. Environmental Health, 24(1), 61.

Smith, K.R., Bruce, N., Balakrishnan, K., Adair-Rohani, H., Balmes, J., Chafe, Z., Dherani, M., Hosgood, H.D., Mehta, S., Pope, D. and Rehfuess, E., 2014. Millions dead: how do we know and what does it mean? Methods used in the comparative risk asseshealsment of household air pollution. Annual review of public health, 35(1), pp.185-206.

Stanke, C., Kerac, M., Prudhomme, C., Medlock, J., and Murray, V. (2013). Health effects of drought: a systematic review of the evidence. PLoS currents

UNDP (2018). Climate Change and the Rise of Poverty (Blog). United Nations Development Programme.

UNICEF. (2023). The impact of disasters on agriculture and food security: Avoiding and reducing losses through investment in resilience-2023.

United Nations Children's Fund, and World Health Organization. (2024). Progress on household drinking water, sanitation and hygiene 2000-2022: special focus on gender. World Health Organization.

Van Donkelaar, A., Hammer, M.S., Bindle, L., Brauer, M., Brook, J.R., Garay, M.J., Hsu, N.C., Kalashnikova, O.V., Kahn, R.A., Lee, C. and Levy, R.C., 2021. Monthly global estimates of fine particulate matter and their uncertainty. Environmental Science and Technology, 55(22), pp.15287-15300.

Vicente-Serrano, S. M., Beguería, S., and López-Moreno, J. I. (2010). A multiscalar drought index sensitive to global warming: the standardized precipitation evapotranspiration index. Journal of climate, 23(7), 1696-1718.

Winsemius, H. C., Jongman, B., Veldkamp, T. I., Hallegatte, S., Bangalore, M., and Ward, P. J. (2018). Disaster risk, climate change, and poverty: assessing the global exposure of poor people to floods and droughts. Environment and Development Economics, 23(3), 328-348.

World Bank. (2025). Climate Change Knowledge Portal: Observed Climate Data, ERA5 0.25-Degree, accessed 20 April 2025.

World Bank (2024). Poverty, Prosperity, and Planet: Pathways Out of the Polycrisis. World Bank.

World Food Programme (2023), Horn of Africa hunger crisis pushes millions to the brink.

World Health Organization. (2024, July 24). Drought.

Yamano, T., Alderman, H., and Christiaensen, L. (2005). Child growth, shocks, and food aid in rural Ethiopia. American Journal of Agricultural Economics, 87(2), 273-288.

Yazdi, M.S., Ardalan, M.A., Hosseini, M., Zoshk, M.Y., Hami, Z., Heidari, R., Mosaed, R. and Chamanara, M., 2024. Infectious diarrhea risks as a public health emergency in floods; a systematic review and meta-analysis. Archives of Academic Emergency Medicine, 12(1), p.e46.

Zhao, Q., Guo, Y., Ye, T., Gasparrini, A., Tong, S., Overcenco, A., Urban, A., Schneider, A., Entezari, A., Vicedo-Cabrera, A.M. and Zanobetti, A. (2021). Global, regional, and national burden of mortality associated with non-optimal ambient temperatures from 2000 to 2019: a three-stage modelling study. The Lancet Planetary Health, 5(7), e415-e425.

Zivin, J. G., and Neidell, M. J. (2014). Temperature and the allocation of time: Implications for climate change. Journal of Labor Economics, 32(1), 1–26.